Agile wide-angle beam steering with electrowetting microprisms

Neil R. Smith[*], Don C. Abeysinghe[*], Joseph W. Haus[#], and Jason Heikenfeld[*]

[*]*Novel Devices Laboratory, University of Cincinnati, Cincinnati, OH 45221.*
[#]*Electro-Optics Program, University of Dayton, Dayton, Ohio 45469.*
jason.c.heikenfeld@uc.edu

Abstract: A novel basis for beam steering with electrowetting microprisms (EMPs) is reported. EMPs utilize electrowetting modulation of liquid contact angle in order to mimic the refractive behavior for various classical prism geometries. Continuous beam steering through an angle of 14° (±7°) has been demonstrated with a liquid index of n=1.359. Experimental results are well-matched to theoretical behavior up to the point of electrowetting contact-angle saturation. Projections show that use of higher index liquids (n~1.6) will result in steering through ~30° (±15°). Fundamental factors defining achievable deflection range, and issues for Ladar use, are reviewed. This approach is capable of good switching speed (~ms), polarization independent operation, modulation of beam field-of-view (lensing), and high steering efficiency that is independent of deflection angle.

©2006 Optical Society of America

OCIS codes: (010.1290) Atmospheric optics; (230.2090) Electro-optical devices; (230.5480) Prisms; (010.3310) Laser beam transmission; (010.3640) Lidar.

References and links

1. A. V. Jelalian, *Laser Radar Systems*, Artech House, Boston-London 1992.
2. J. D. Zook, "Light beam deflector performance: a comparative analysis," Appl. Opt. **13**, 875-887 (1974).
3. L. Sun, J. H. Kim, C. H. Jang, D. C. An, X. J. Lu, Q. J. Zhou, J. M. Taboada, R. T. Chen, J. J. Maki, S. N. Tang, H. Zhang, W. H. Steier, C. Zhang, and L. R. Dalton, "Polymeric waveguide prism-based electro-optic beam deflector," Opt. Eng. **40**, 1217-1222 (2001).
4. B. D. Duncan, P. J. Bos and V. Sergan, "Wide-angle achromatic prism beam steering for infrared countermeasures," Opt. Eng. **42**, 1038-1047 (2003).
5. J. L. Gibson, B. D. Duncan, E. A. Watson and J. S. Loomis, "Wide-angle decentered lens beam steering for infrared countermeasures applications," Opt. Eng. **43**, 2312-2321 (2004).
6. P. F. McManamon, T. A. Dorschner, D. L. Corkum, L. J. Friedman, D. S. Hobbs, M. Holz, S. Liberman, H. Q. Nguyen, D. P. Resler, R. C. Sharp, and E. A. Watson, "Optical Phased Array Technology," Proc. IEEE **84**, 268-298 (1996).
7. P. F. McManamon, "Agile Nonmechanical Beam Steering," Opt. and Phot. News, **17,** 25-29 (2006).
8. O. Pishnyak, L. Kreminska, O. D. Lavrentovich, J. J. Pouch, F. A. Miranda, B. K. Winker, "Liquid crystal digital beam steering device based on decoupled birefringent deflector and polarization rotator," Mol. Crys. and Liq. Crys. **433**, 279-295 (2005).
9. B. Winker, M. Mahajan, M. Hunwardsen, "Liquid crystal beam directors for airborne free-space optical communications," in Proc. of IEEE Conf. on Aerospace **3,** 1702-1709 (2004).
10. F. Mugele and J. C. Baret, "Electrowetting: From basics to applications," J. Phy. Condens. Matter **17**, R705-R774 (2005).
11. B. Berge and J. Peseux, "Variable focal lens controlled by an external voltage: An application of electrowetting," Euro. Phys. J. E **3**, 159-163 (2000).
12. S. Kuiper and B. H. W. Hendriks, "Variable-focus liquid lens for miniature cameras," Appl. Phys. Lett. **85**, 1128-1130 (2004).
13. R. A. Hayes and B. J. Feenstra, "Video-speed electronic paper based on electrowetting," Nature **425**, 383-385 (2003).
14. J. Heikenfeld and A. J. Steckl, "Intense switchable fluorescence in light wave coupled electrowetting devices," Appl. Phys. Lett. **86,** 011105 (2005).
15. J. Heikenfeld and A. J. Steckl, "Electrowetting Light Valves with Greater than 80% Transmission, Unlimited View Angle, and Video Response," Soc. Inf. Display Symposium Digest **36**, 1674-1677 (2005).

#70225 - $15.00 USD Received 24 April 2006; revised 21 June 2006; accepted 23 June 2006
(C) 2006 OSA

16. S. Kuiper, B. H. W. Hendriks, R. A. Hayes, B. J. Feenstra, and J. M. E. Baken, "Electrowetting-Based Optics," Proc. of SPIE **5908**, 0R1-0R7 (2005).
17. S. Kuiper and B. H. W. Hendriks, L. J. Huijbregts, A. M. Hirschberg, C. A. Renders, M. A. J. van As, "Variable-focus liquid lens for portable applications," Proc. SPIE **5523**, 100-109 (2004).
18. J. Y. Chen, A. Kutana, C. P. Collier, and K. P. Giapis, "Electrowetting in Carbon Nanotubes," Science **310**, 1480-1483 (2005).
19. G. Kaminski, "Micromachining of silicon mechanical structures," J. Vacuum Sci. and Tech. B. **3**, 1015-1024 (1985).
20. F. Mugele, "Electrowetting beyond Lippmann's approximations: field-induced surface distortions and finite conductivity effects in capillary breakup" International Electrowetting Workshop, Rochester, (2006).

1. Introduction

Rapid and accurate repositioning of an optical beam is an essential element for free-space optical communications and laser detection and ranging (Ladar)[1]. In order to continue to advance system-level performance for these applications, it has long been desired to overcome the bulk, cost, slow speed, and lack of agility associated with mechanical beam steering approaches such as the dual-axis gimbaled mirror. These needs have fueled impressive development efforts in finding new approaches for beam steering. Alternative approaches now include acousto-optic[2] and electro-optic polymer [3] devices, decentered prisms and lenses[4,5], optical phased arrays based on dynamic liquid crystal gratings[6,7], and liquid crystal polarization rotators followed by multi-stage birefringent prisms[8,9]. Significant advances have now been made in key performance areas such as size, agility, and power. However, providing wide-angle steering with these new approaches often requires cascading of multiple active and/or passive steering elements. Therefore, wide-angle capability remains to be achieved in a stand-alone electro-optic element. Furthermore, to enable broader use in civilian applications, an electro-optic element is needed which is inherently simpler to fabricate/implement. An excellent candidate technology for next-generation beam steering is liquid optical elements modulated via electrowetting[10]. Presently, most electrowetting optics development is concentrated in the area of tunable liquid lens systems [11,12] and displays [13,14]. Our working group is investigating the feasibility of arrayed electrowetting microprisms (EMPs) for robust Fresnel and phased-array optics. Reported here is the fabrication and demonstration of EMPs with continuous beam steering through an angle of 14° (±7°). This exceeds the continuous steering angles demonstrated for optical phased-array technology. Shown in Fig. 1 are photographs of open-channel EMPs in various states of operation. EMPs are promising for wide-angle steering, good switching speed (~ms), polarization independent operation, modulation of field of view, lensing, and high steering efficiency at all angles.

2. Experiment

A simple EMP fabrication approach was implemented for the experiments reported in this work. It is important to note that for near infrared EMPs implemented in a linear-arrayed format (i.e. Fresnel optic), an alternate fabrication approach using microfabrication/etching of

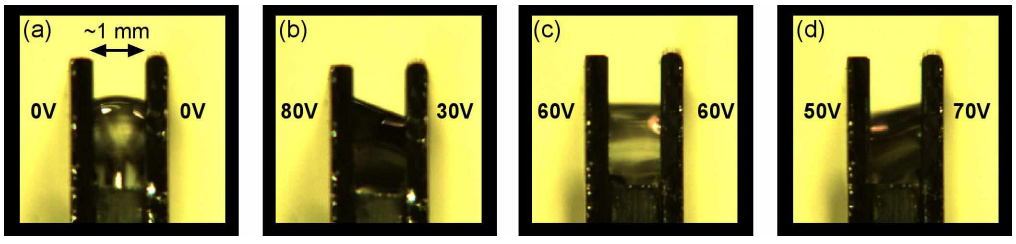

Fig. 1. Side-view photographs of EMPs with (a) zero voltage and (b-d) various voltage/prism configurations. The liquid is electrically grounded and voltages are applied to the side-walls. For photographic purposes these open-channel EMPs lack top and end sealing plates.

#70225 - $15.00 USD Received 24 April 2006; revised 21 June 2006; accepted 23 June 2006
(C) 2006 OSA

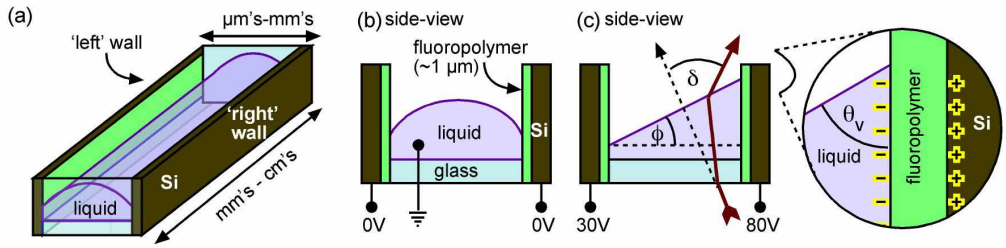

Fig. 2. Angled view diagram (a) of representative channel geometry for EMPs. Side view diagrams (b,c) of basic EMP materials, voltage connections, and angles for prism apex (ϕ), deflection (δ) and liquid-fluoropolymer contact (θ).

silicon-on-insulator substrates would be utilized. The approach reported here is simply a useful technique for rapid characterization of various EMP structures and materials. To begin fabrication, rectangular silicon wafers were thermally oxidized with 100 nm of SiO_2. These wafers were then dip coated in 2 wt.% fluoropolymer solution. Exemplary fluoropolymer solutions include DuPont Teflon AF in fluorosolvent. After baking at ~160 °C a solid hydrophobic insulator film of ~1 μm thickness, ε_r~1.9, and surface energy of γ~16 dynes/cm was formed. Although the fluoropolymer itself is electrically insulating (>1 MV/cm), it is slightly porous and benefits from the additional electrical insulation provided by the underlying thin oxide layer. As shown in Fig. 2, EMPs were formed by bonding two of these completed substrates to a transparent glass spacer. For a sealed-channel device, this spacer is treated or textured to increase its surface energy. This hydrophilic surface is desired to promote filling of the EMP channel with an aqueous solution. Completed EMP channels were partially filled with a water:glycerin:KCl solution of 80:20:0.1 mixture by weight. The surface tension of the mixture is very close to that of pure water (γ~73 dynes/cm). The glycerin has higher refractive index (n=1.47) while also reducing solution evaporation rate. The KCl provides proper electrical conductivity. Using an Abbe refractometer, the refractive index of this mixture was found to be n=1.359. A glass spacer width of ~1 mm or less was used to alleviate gravitational effects on the curvature of the liquid meniscus. In order to allow larger-size devices, electrowetting optics [12-15] often utilize an additional non-polar liquid (oil) that is density matched to the aqueous solution. This was also investigated with EMPs and was found to allow EMPs with channel spacing approaching ~5 mm. One independent DC voltage source was attached to each Si side-wall, while the channel liquid was held at 0V by the insertion of an electrically grounded Ni-Ti wire. A beam source was provided by a 633 nm HeNe laser beam with surface-normal incidence and centering onto the glass spacer. Beam diameter was reduced to fit completely inside the channel so that side-wall interference was eliminated. Deflection was calculated from laser spot location at a distance of ~2 m past the EMP. It is important to note that liquid geometry in the channel can take on a spherical or cylindrical wetting/meniscus configuration based on the geometry and surface energies of the side-walls, top plate, end sealing plates, and additional features (not shown). Long-channel EMPs require a cylindrical geometry. Techniques for long-channel EMP fabrication, such as a new pivoted EMP design, will be reported later.

3. Electrowetting control of prism apex angle

The liquid contact angle is readily translated to the prism apex angle in our device geometry. The electrowetting equation[10] relates the response of liquid/solid contact angle to an externally applied electrical potential. The parallel-capacitor liquid/dielectric approximation for the electrowetting equation applies to this work:

$$\cos(\theta_V) = \cos(\theta_0) + \frac{1}{2} \cdot \frac{\varepsilon \cdot V^2}{\gamma \cdot d} \qquad (1)$$

#70225 - $15.00 USD Received 24 April 2006; revised 21 June 2006; accepted 23 June 2006
(C) 2006 OSA

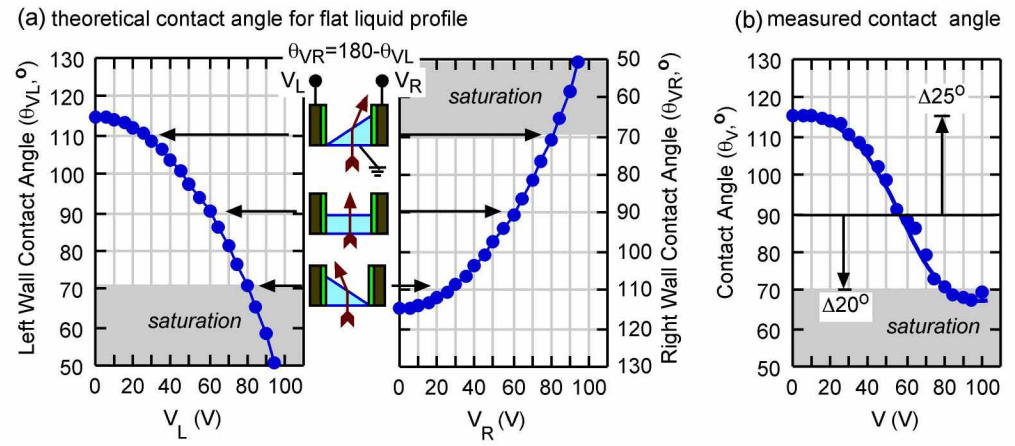

Fig. 3. Plot of (a) theoretical contact angle vs. voltage for left (θ_{VL}) and right (θ_{VR}) EMP sidewalls and (b) experimentally measured contact angle vs. voltage. The diagrams and double-plot in (a) emphasize the need for symmetric contact angle inversion, and can be used to determine the applied voltages required for various EMP apex angles. Experimentally observed contact angle saturation at θ~70° is grey-shaded in the diagrams. This limits the steering capability of the EMP. Used only for descriptive purpose, the terms 'left' and 'right' voltages/walls can be referenced back to Fig. 2(a).

Here, θ_0 is the contact angle without externally applied electrical potential, θ_V is the contact angle under an electrical potential of V, ε is the electric permittivity of the dielectric layer beneath the droplet, γ is the liquid surface tension, and d is the thickness of dielectric layer. EMP modulation can be described as follows. As shown in Fig. 2(b), when placed between conducting plates coated with hydrophobic dielectric the polar liquid forms a convex shaped meniscus due to a large liquid-fluoropolymer contact angle (θ_0~115°). Through application of a voltage (charge) across the hydrophobic fluoropolymer dielectric, Fig. 2(c), the effective interfacial surface tension between the liquid and fluoropolymer decreases, resulting in a decrease in contact angle (θ_V). Contact angle is related to prism apex angle (φ) according to $\varphi = |90° - \theta_V|$. In order to obtain a straight-line meniscus from side-wall to side-wall, Fig. 2(b), the contact angles on both the left (θ_{VL}) and right (θ_{VR}) sides should be inverted about 90° contact ($\theta_{VR} = 180 - \theta_{VL}$). For example, if the right wall of Fig. 2(b) were biased at ~80V such that θ_{VR}=70°, then the contact angle on the left side should be θ_{VL}=110° which requires a left wall bias of ~25V. This requirement for contact angle symmetry is visualized graphically in Fig. 3(a) (theory, Eq. 1). For any given apex angle, a horizontal line can be drawn across both plots and the required voltages obtained. Experimentally measured contact angle vs. voltage tracks-well with theory and is plotted in Fig. 3(b). However, in agreement with other investigations[10], presently available liquids and fluoropolymers limit contact angle reduction to saturation at θ_V ~70°. Electrowetting saturation at θ_V ~70° is 5° short of the inverse apex angle that can be achieved in the dewetted state (θ_0~115°). Considering the EMP requirement for symmetry of contact angle inversion, the usable range for contact angle is therefore limited to 70° through 110°. θ_0 can be increased through increased liquid surface tension or reduced dielectric surface energy (increased hydrophobicity). Both hydrophobicity and wetting saturation are therefore topics of future research interest. The higher voltage range (0-100V) utilized for the EMPS is due the low capacitance of the fluoropolymer dielectric. Operation voltage can be reduced through use of higher capacitance dielectrics. This has been demonstrated for low-voltage (0-16V) electrowetting displays [15].

4. Electrowetting control of prism beam steering

The refractive property of prisms and their ability to deviate a beam of light that passes through them is well known. To illustrate possible steering angles through modulation of EMP apex angle, the angular deviation (δ) of a light beam passing through a prism with an

#70225 - $15.00 USD Received 24 April 2006; revised 21 June 2006; accepted 23 June 2006
(C) 2006 OSA

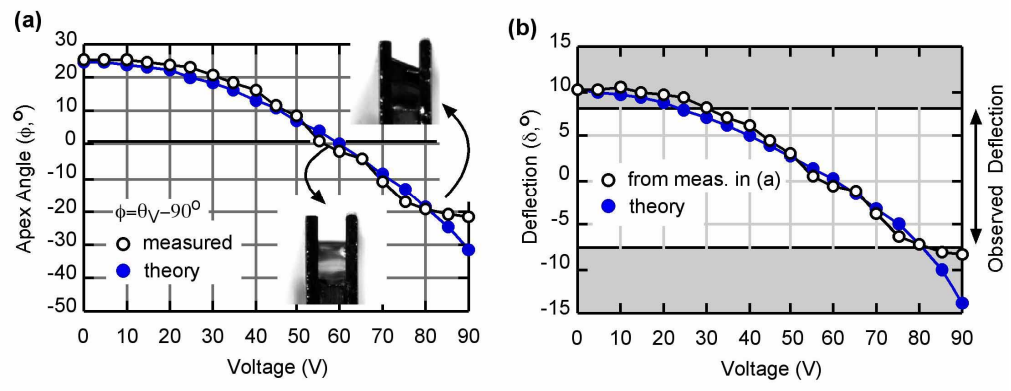

Fig. 4. Plots of (a) apex angle and (b) beam deflection vs. voltage. Apex angle can be directly related to applied voltage using Eq.1. Deflection can then be related to apex angle using Eq. 2.

index of refraction n>1, apex angle φ, and angle of incidence α_i (0° in our case) can be expressed as:

$$\delta = \alpha_i - \phi + \sin^{-1}\left[\left(n^2 - \sin^2\alpha_i\right)^{1/2}\sin\phi - \cos\phi\sin\alpha_i\right] \quad (2)$$

Apex angle and deflection angle can be related by Eq. 2 and are plotted in Fig. 4(a), 4(b), respectively. As shown in Fig. 4(b), actual observed laser deflection was +7° to -7° (14° total continuous). The detraction from the curve for theoretical deflection is due to the constraint of a symmetrically inverted contact angle (Fig. 3, and related discussion). For the data in Fig. 4(b), voltage for only one side-wall is labeled. As previously discussed, corresponding voltages on the opposing wall can be obtained from Fig. 3. Additional control over the beam profile (lensing) can be achieved by implementing non-symmetric contact angles [16]. With the EMPs, simultaneous voltage control of steering angle and beam profile was observed. Total continuous deflection angle (2δ) measured via laser spot location is plotted vs. voltage in Fig. 5(a). Steering results greater than 14° (-7° to +7°) were not observed as predicted, which is due to contact angle saturation. For these measurements, DC applied voltages were utilized. In future work, devices will be tested with all-electrical feedback controls and biased with AC voltages at frequencies greater than the EMP response time. Feedback control circuitry is essential for high-accuracy beam steering. AC voltage is expected to reduce contact angle hysteresis and improve maximum deflection slightly beyond the presently observed limit of ~14°. A straightforward route to increased steering angle is to increase the refractive index of the liquid. A theoretical plot of total continuous deflection vs. apex angle for n=1.36 (this work) and n=1.60 is provided in Fig. 5(b). Aqueous solutions of heavy-metal salts can achieve n>1.5. High salt concentration is also advantageous for widening the usable temperature range. Water is desirable as the primary solvent since it is light-stable, has high surface tension, and has low viscosity. Lower surface tension liquids have reduced contact angle at zero-voltage (θ_0) and therefore complicate design due to the symmetry requirement for apex angle. An oil/water system is also an attractive option. Although the index contrast for water/oil can be lower than that of water/air, a water/oil EMP system is likely to achieve a larger range of contact angle change[10]. Another alternate route is to scale the technology down to a diffractive approach using arrayed capillary electrowetting device structures. This approach functions similar to the step-indexing approach used in liquid crystal phased-arrays. As shown at the right of the vertical dotted line in Fig. 5(b), the effective apex angle can then increase substantially, but with likely consequence of reduced steering efficiency.

#70225 - $15.00 USD Received 24 April 2006; revised 21 June 2006; accepted 23 June 2006
(C) 2006 OSA

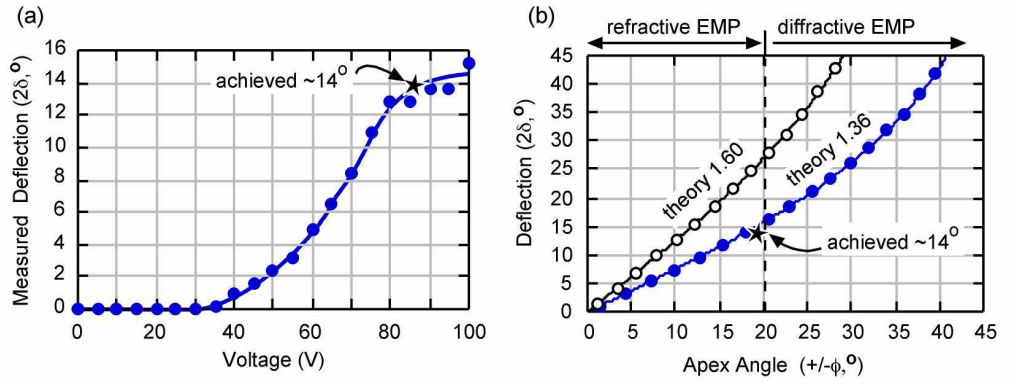

Fig. 5. Plot of (a) total continuous beam deflection vs. voltage as measured by laser spot location, (b) theoretical total deflection predicted for liquid of n=1.36 (this work) and for n=1.60.

5. Discussion on potential use for Ladar systems

Initial tests and theoretical predictions clearly show the superior performance of EMPs with respect to their maximum steering angle as compared to other single-plate electrically-controlled beam steering approaches. Furthermore, as electrowetting devices are scaled down in size, switching speeds are theoretically projected to reach 10's of kHz. Switching speed increases rapidly with decreasing liquid volume according to $\tau \propto (\rho \times v/\gamma)^{1/2}$, where $\rho \times v$ is the density-volume product [17]. Recently, electrowetting inside a carbon nanotube has been achieved and a ~1ns (GHz) electrowetting speed suggested [18]. For high-accuracy applications, one will need to further factor in delay due to feedback controls. For Ladar applications, high power lasers are often utilized and it is very important to address the issue of device aperture. Large EMP apertures are desired so that expanded beams can reduce the laser power density well-below the laser damage threshold. Since larger scale EMPs will become slower and more susceptible to gravity, a large aperture should be achieved by implementing numerous small EMPs in arrayed format. A proposed structure for arrayed EMPs in a Si-on-oxide substrate is presented in Fig. 6. Presently utilized materials systems (liquids, Si, fluoropolymer) are compatible with lasers in the 1-2 μm spectral window. Longer wavelength systems (~10 μm) will require both new materials and scale down of EMP thickness in order to reduce attenuation. EMPs are inherently capable of steering light of any polarization. However, liquid optics are often more dispersive than their solid-phase counterparts. Therefore, using a water/oil electrowetting system as an optical doublet is proposed for dispersion-sensitive applications such as image steering. A two-liquid water/oil system is also advantageous if the liquids are density matched. Density matched liquids eliminate vibration, gravity, and acceleration effects. This is critical for coupling of the technology with air and ground vehicles. Even though using two liquids reduces index contrast and maximum deflection capability, large changes in switchable contact angle are possible for water/oil systems [10]. Aqueous solutions or high index silicone oils can achieve refractive indices approaching n~1.6. Coupled with a low index counter liquid an index contrast of ~0.3 might be obtainable. A second option that allows single liquid use and high index contrast (>0.5), is to counter-act vibration/acceleration by scaling-down EMP size. At sub-mm dimensions gravity and conventional acceleration effects are mitigated. As micro-scale dimensions are reached even strong vibration has less impact on EMP operation. This simply because as size decreases, surface-tension forces dominate over force due to mass and acceleration. The dominance of surface tension over gravitational force can be quantified as the Bond Number, $B_0=(g \cdot \Delta\rho \cdot R^2/\gamma)^{1/2}$ [10]. Scaling down the EMP size is also desirable since the switching speed increases and the power handling capability increases; i.e. scaling down allows EMPs to be distributed in 1D arrayed format for use with expanded beams.

#70225 - $15.00 USD Received 24 April 2006; revised 21 June 2006; accepted 23 June 2006
(C) 2006 OSA

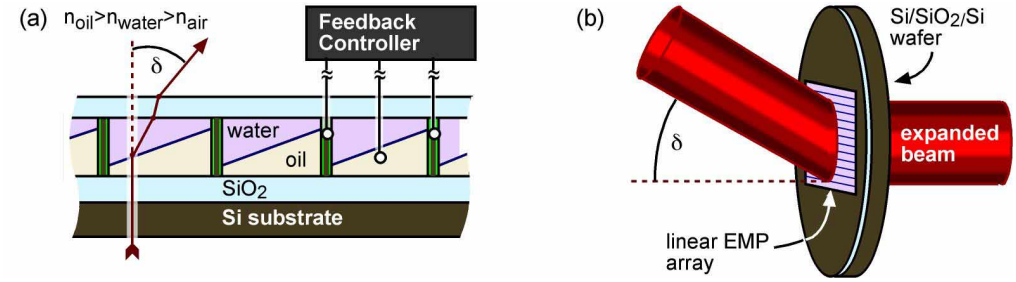

Fig. 6. Diagrams of (a) proposed approach for fabricating arrayed EMP's in Si-on-oxide substrates, and (b) use of arrayed EMPs in order to allow increased laser beam power by expanding the beam (reduced power density). As noted diagrammatically in (a), refraction at all interfaces should be considered when calculating the total beam deflection.

Furthermore, linear scale down in terms of EMP thickness (optical path length) reduces absorption. Operating in a Fresnel format, steering efficiency is preserved even at wide steering angles. This is because side-wall reflection is minimized as the top-refractive surface is brought close to the top of the side-wall corresponding to the steering direction. The fill factor can be quite high using demonstrated Si side-wall etching techniques. For an EMP that is 50 microns high, a switchable apex angle of 20° translates to a width of 137 μm. If one assumes a 40:1 Si wall aspect ratio[19] with 0.5 microns hydrophobic dielectric thickness, the calculated fill factor is ~ 98%. Considering fabrication challenges, a goal of >90-95% is likely more realistic. A phased-array approach is even theoretically possible with further EMP scale down. For example, an index contrast of n=0.3 and operation at 1.06 μm, would require an EMP height of 3.53 μm and a 9.71 μm pitch. However, fill factor becomes a larger issue for a phased-array since thin side-wall fabrication becomes more challenging. One further needs to address the effect of diffraction from the arrayed Si sidewalls. This undesired diffraction will limit the steering efficiency. Also, at small dimensions one must consider the presence of a thin (<1 μm), but non-zero thickness of oil film between the water and fluoropolymer [20]. A wide 1D EMP array could be controlled using only two switching voltage sources and two static voltage sources. Electrically, this is much simpler than the numerous electrodes required for step-indexing the refractive index profile of electro-optic materials. Issues such as steering efficiency, feed-back controls for steering accuracy, contact angle hysteresis, and fabrication scale-down, remain to be addressed. However EMPs have the potential to provide compelling beam-steering advantages in wide-deflection angle, high speed, low driving voltages/power, inherent dispersion correction, polarization independence, simple control circuitry, and high optical power.

Acknowledgments

The authors acknowledge technical support for this work by Dr. Paul F. McManamon and financial support from the Air Force Research Laboratory.

#70225 - $15.00 USD Received 24 April 2006; revised 21 June 2006; accepted 23 June 2006
(C) 2006 OSA